Molecular Simulation, 2004 Vol. 30 (5), 30 April 2004, pp. 289-300

Taylor & Francis
Taylor & Francis Group

Estimation of the Binding Energy in Random Poly (Butylene terephtalate-*co*-thiodiethylene terephtalate) Copolyesters/Clay Nanocomposites via Molecular Simulation

MAURIZIO FERMEGLIA*, MARCO FERRONE and SABRINA PRICL

Computer-aided Systems Laboratory, Department of Chemical Engineering-DICAMP, University of Trieste, Piazzale Europa 1, I-34127 Trieste, Italy

(Received ????; In final form November 2003)

Molecular mechanics/dynamics computer simulations are used to explore the atomic scale structure and to predict binding energy values for polymer/clay nanocomposites based on random poly(butylene terephtalate-*co*-thiodiethylene terephtalate) copolyesters, montmorillonite and several, different organic surfactant. Our results reveal that the energy of binding between the polymeric matrix and the montmorillonite platelet shows a decreasing trend with increasing molecular volume, *V*, of the organic compounds used as surfactant, and that the substitution of hydrogen atoms with a –SH moiety in the organic molecules results in progressively increasing interaction of the surfactant with the copolymer, as the sulfur-containing comonomer concentration is increased. Finally, under the hypothesis that the clay platelets are uniformly dispersed within the polymer matrix, the pristine clay still yields a high interfacial strength between MMT and copolymers.

Keywords: Nanocomposites; Sulfur-containing copolymers; Molecular simulations; Polymer-organoclays; Binding energies

INTRODUCTION

The *in situ* formation and assembly of silicate nanoparticles with high aspect ratio represent the key to novel structural and functional polymeric materials with skeleton-like silicate superstructures. In contrast to conventional filled polymers, a few percent of *in situ* formed nanosilicates are sufficient to improve significantly polymer properties without encountering dispersion problems and health hazards associated with the handling of prefabricated needle- and whisker-like nanoparticles. The *in situ* nanocomposite is of particular interest to upgrade and diversifying existing polymers. Enthusiastic business forecasts claim billion dollar opportunities for the development of nanocomposites with applications ranging from light-weighted automotive engineering plastics with increased stiffness/toughness performance and higher heat distortion, to reinforced transparent glasses, barrier resins, low-stress advanced structural materials, halogen-free flame retardant coatings, polyelectrolyte membranes for fuel cells and batteries, and even novel light-emitting diodes [1–4]. Although some reports glorify the discovery of these nanocomposites as revolutionary breakthrough in science and technology, it should be noted that the basic synthetic concept has been established since the 1980s. Indeed, the pioneering work by researchers from Toyota [5–9], who discovered the possibility to build a nanocomposite from polyamide-6 and montmorillonite, the renewed interest in chemical nanotechnology, and the quest for upgrading of old polymers, have fueled nanocomposite development.

Among all potential nanocomposite precursors, those based on clay and layered silicates have been more widely investigated, probably because of the abundant availability of the clay materials, and because their intercalation chemistry has been know for a long time [10]. Depending on the nature of the components used and the method of preparation, basically three main types of composites may be obtained when a layered clay is associated with

*Corresponding author. Tel.: +39-040-558-3438. Fax: +39-040-569823. E-mail: mauf@dicamp.units.it

ISSN 0892-7022 print/ISSN 1029-0435 online © 2004 Taylor & Francis Ltd
DOI: 10.1080/08927020410001659385

a polymer. When the polymer is unable to intercalate between the silicate sheets, a phase-separated composite is obtained, whose properties stay in the same range as traditional microcomposites. Beyond this classical family, two other types of nanocomposites can be recovered. Intercalated structures, in which a single (or more than one) extended polymer chain is intercalated between the silicate layers, resulting is a well ordered multilayer morphology, built up with alternating polymeric and inorganic layers. When the silicate layers are completely and uniformly dispersed in a continuous polymeric matrix, an exfoliated or delaminated structure is obtained.

Factors limiting successful dispersion of the layered silicates are the hydrophilic nature of the silicates and the largely hydrophobic nature of most engineering polymers. To produce an intercalated nanocomposite, the polymer has to wet the clay particles to some extent so that the polymer chains are intercalated between the clay galleries. To make delaminated or exfoliated nanocomposites, a higher degree of wetting is required.

Fabricating these materials in an efficient and cost-effective manner, however, poses significant synthetic challenges. To understand these challenges, it is useful to consider the structure of the clay particles. The layered silicates commonly used in nanocomposites (montmorillonite being a prime example) belong to the structural family known as the 2:1 phyllosilicates. Their crystal lattice consists of 2-D layers where a central octahedral sheet of alumina or magnesia is fused into two external silica tetrahedron by the tip, so that the oxygen ions of the octahedral sheet do also belong to the tetrahedral sheet. These layers organize themselves to form stacks with a regular van der Waals gap in between them, called interlayer or gallery. Isomorphic substitution of some elements within the layers—e.g. Al^{3+} with Mg^{2+}, or Mg^{2+} with K^{+}—generates negative charges that are counterbalanced by alkali or alkaline earth cations situated in the interlayers. The lateral dimensions of these layers may vary from approximately 300 Å to several microns or more, depending on the peculiar composition of the silicate, while the spacing between the closely packed sheets is also of the order of 1 nm, which is smaller than the radius of gyration of typical polymers. Consequently, there is a large entropic barrier that inhibits the polymer from penetrating this gap and becoming intermixed with the clay.

Thus, there are several issues that need to be addressed in order to optimize the production of these polymer–clay nanocomposites (PCNs). Of foremost importance is isolating conditions that promote the penetration of the polymer into the narrow gallery. If, however, the sheets ultimately phase-separate from the polymeric matrix, the mixture will not exhibit the improved strength, heat resistance, or barrier properties. Therefore, it is also essential to determine the factors that control the macroscopic phase behavior of the mixture. Finally, the properties of the hybrid commonly depend on the structure of the material; thus, it is of particular interest to establish the morphology of the final composite.

To enhance polymer–clay interaction, the clay interlayer surfaces of the silicate are chemically treated to make the silicate less hydrophilic and therefore more wettable by the polymer. A cation exchange process accomplishes this, where hydrophilic cations such as Na^{+}, K^{+} or Ca^{++} are exchanged by a surface modifier, usually selected from a group of organic substances having an alkyl radical containing at least 6 carbon atoms. The role of this organic component in organosilicates is to lower the surface energy of the inorganic host and improve the wetting characteristic with the polymer. Intuitively, the nature and the structure of these "surfactants" determines the hydrophobicity of silicate layers and, hence, the extent of their exfoliation.

Indeed, the driving force for nanodispersion—that is the negative change in free energy—depends on the delicate balance between the enthalpic term, due to the intermolecular interactions, and the entropic term, associated with the configurational changes in the constituents. Using a recently developed mean-field model [1], it has been shown that the entropy loss associated with the polymer confinement is approximately compensated by an entropy gain associated with the increased conformational freedom of the surfactant molecules as the gallery distance increases due to the polymer intercalation. Therefore, enthalpy determines whether or not polymer intercalation will take place.

From the foregoing discussion it might be inferred that, because of the major role played by the clay surface modification in the thermodynamics of nanoformation, not all organic components are equally effective. Indeed, some compounds might result to be incompatible with the polymeric matrix, as well as some others may not be able to increase the gallery dimensions at all.

In recent years, the synthesis and study of the related properties of sulfur-containing polyesters have received a renewed impulse, due to some specific applications proposed for these materials. Indeed, several papers evidence that the presence of sulfur atoms in a polymeric chain can increase some important properties, including their biodegradability. Moreover, it is well known that copolymerization represents an easy way to modify the characteristics of a polymer in order to fit specific applications; for instance, the degree of crystallinity and melting point can be adjusted by random

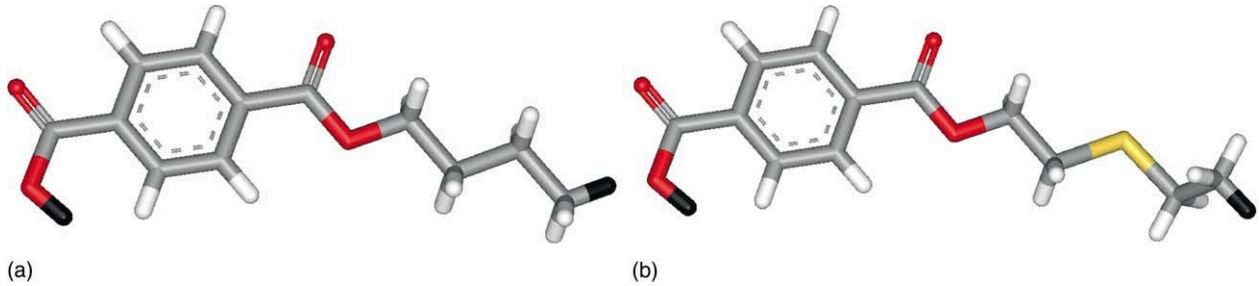

FIGURE 1 Comonomeric units of the poly(butylene terephtalate-*co*-thiodiethylene terephtalate). (left) BT; (right) TDET.

copolymerization and by changing copolymer composition. As a consequence, several copolyesters containing sulfur in the main or in side chains were recently prepared and studied [11–15]. Under this view, and due to the widespread use of poly(butylenes terephtalate) (PBT), a well-known thermoplastic material with good properties for an ever growing number of applications, Lotti *et al.* recently synthesized and characterized a series of random copolyesters of PBT by direct melt polymerization, starting from dimethylenterephtalate, 1,4-butanediol and thiodiethylene glycol (Fig. 1) [16].

Composition appears to be the prominent parameter in determining the characteristics of the polymeric materials: the main effect of copolymerization is a lowering in the amount of crystallinity and a decrease of melting temperature with respect to homopolymers. In particular, amorphous samples (containing 50–100 mol% of thiodiethylene terephtalate units) show a monotonic decrease of the glass transition temperature as the content of sulfur-containing units is increased, due to the presence of the flexible C–S–C bonds in the polymeric chains.

Since the presence of the sulfur atoms constitutes a prerequisite for the biodegradability of these copolyesters [17] but, at the same time, results in the lowering of the overall performances of the corresponding macromolecules, we considered that a combination of the potentially environmentally benign properties of these polymers with the high strength and stability of the clay (another abundant, economic and environmentally friendly material) could be an interesting realization. To this purpose, and since there are no reports on the preparations of nanocomposites from these sulfur-containing polyesters, we decided to perform a preliminary investigation on which, among a small list of selected compounds, would be the most effective in providing stronger interactions and high interfacial strength between the disperse clay platelets and the copolyesters.

Following a very recent approach [18,19], we applied force-field based, atomistic molecular dynamics (MD) simulations for the calculation of binding energies between all polymer/organoclay components. The basic machinery of the procedure consists in building a molecular model comprising three copolyesters, characterized by a different content of sulfur-containing units, a given surfactant and a MMT platelet, refining and equilibrating it by molecular mechanics/MD, and calculating the binding energies as guidelines for screening among different intercalant surface modifiers to make sulfur-containing copolyester CNs characterized by a strong interface between dispersed clay platelets and the copolymeric matrix.

COMPUTATIONAL DETAILS

In accordance to previous work [18,19], a simplified model, assuming all MMT platelets to be at low volume concentration and fully dispersed in the polymeric matrix so that they do not interact each other, consists of copolyester molecules interacting with surfactants and exposed silicate surface on one side of a MMT clay platelet.

As most of minerals, montmorillonite is present in nature with a variety of chemical compositions and structural features; nonetheless, both properties can be considered as derived from those of pyrophyllite by random substitution of Al by Mg ions [20]. Basically, pyrophyllite is made up by a 2-D array of aluminum–oxygen–hydroxyl octahedra packed between two 2-D arrays of silicon–oxygen tetrahedra, resulting in a three layer platelet. Thus, starting from the relevant crystallographic coordinates [21], we built the unit cell of a pyrophyllite crystal using the Crystal Builder modulus of the Materials Studio molecular modeling package (v 2.2, Accelrys, San Diego, CA, USA). To obtain the corresponding crystal structure of MMT, some aluminum ions were substituted by magnesium ions. The resulting lattice is monoclinic, with space group $C2/m$, and characterized by the following lattice parameters: $a = 5.20$ Å, $b = 9.20$ Å, $c = 10.13$ Å and $\alpha = 90°$, $\beta = 99°$ and $\gamma = 90°$.

Several intercalant surface modifiers of different nature were considered in this study, and are reported in Table I. Some of such compounds are commercially available, other can be synthesized. Due to the slightly polar nature of the copolyesters

TABLE I Chemical formula, acronyms and names of intercalant surface modifiers

Chemical formula	*Acronym*	*Name*
Pristine	Pristine	
$C_{12}H_{27}N$	DDAm	Dodecylamine
$C_{18}H_{39}N$	ODAm	Octadecylamine
$C_{12}H_{24}O_2$	Lac	Dodecanoic (lauric) acid
$C_{18}H_{36}O_2$	Sac	Octadecanoic (stearic) acid
$H_2NC_{12}H_{23}O_2$	LAc-1A	Dodecanoic (lauric) acid, 1-amino
$H_2NC_{18}H_{35}O_2$	SAc-1A	Octadecanoic (stearic) acid, 1-amino
$HSC_{12}H_{23}O_2$	LAc-1T	Dodecanoic (lauric) acid, 1-thio
$HSC_{18}H_{35}O_2$	SAc-1T	Octadecanoic (stearic) acid, 1-thio
$HSC_{12}H_{26}N$	DDAm-1T	Dodecylamine-1-thio
$HSC_{18}H_{38}N$	ODAm-1T	Octadecylamine-1-thio
$C_{16}H_{30}NONH_2$	ADDP	*N*-(12-aminododecyl)-2-pyrrolidone
$C_{22}H_{42}NONH_2$	AODP	*N*-(18-aminooctadecyl)-2-pyrrolidone
$C_{16}H_{30}NOCOOH$	LADP	*N*-(12-carboxydodecyl)-2-pyrrolidone
$C_{22}H_{42}NOCOOH$	SADP	*N*-(18-carboxyoctadecyl)-2-pyrrolidone
$C_{16}H_{30}NOSH$	TDP	*N*-(12-thiododecyl)-2-pyrrolidone
$C_{22}H_{42}NOSH$	TOP	*N*-(18-thiooctadecyl)-2-pyrrolidone

considered, in principle organic modifiers bearing polar substituents could be expected to exhibit enhanced compatibility with the polymeric matrix. Accordingly, to verify this hypothesis some $-NH_2$, $-COOH$ or $-SH$ groups have been introduced in the structure of the compounds, in the chain terminal position.

The model structures of all surface modifiers were generated using the sketcher tool of Materials Studio. All the molecules were subjected to an initial energy minimization using the Compass force field [22,23] of Discover, the convergence criterion being set to 10^{-4} kcal/mol Å. Probably, the most crucial and important aspect of these calculations is the way we selected to sample the relevant configurational phase-space. Accordingly, the conformational search was carried out using a combined molecular mechanics/molecular dynamics simulated annealing (MDSA) protocol [24], in which the relaxed structures were subjected to 5 repeated temperature cycles (from 350 to 700 K and back) using constant volume/constant temperature (NVT) MD conditions. At the end of each annealing cycle, the structures were again energy minimized to converge below 10^{-4} kcal/mol Å, and only the structures corresponding to the minimum energy were used for further modeling. The electrostatic charges for the geometrically optimized organic molecules were obtained by restrained electrostatic potential (RESP) fitting [25,26], and the electrostatic potentials were produced by single-point quantum mechanical calculations at the Hartree–Fock level with a 6-31 + G* basis set [27].

The generation of accurate model amorphous structures for three poly(butylene terephtalate-*co*-thiodiethylene terephtalate) (BT/TDET) copolyesters, having composition 80/20, 50/50 and 20/80 mol%, respectively, was conducted as follows. First, the constitutive repeating units (CRUs) was built and their geometry optimized by energy minimization again using the COMPASS force field. Hence, the appropriate number of each CRU was randomly copolymerized to a conventional degree of polymerization (DP) equal to 30. Although this chain may be too short to capture the genuine response of a long copolyester molecule, in the case of polystyrene it has been verified that a polymer with the same DP is longer than the average physisorbed train size of PS in PCNs [28]. Explicit hydrogen were used in all model systems. The Rotational Isomeric State (RIS) algorithm [29,30], at $T = 350$ K, was used to create the initial conformation of each copolymer. The structure was then relaxed to minimize energy and avoid atom overlaps using the conjugate-gradient method.

Such a straightforward molecular mechanics scheme is likely to trap the simulated system in a meta-stable local high-energy minimum. To prevent the system from such entrapments, the relaxed structure was subjected to the same MDSA protocol applied to model the organic components. At the end of each annealing cycle, the structure was again relaxed via FF, using a rms force less than 0.1 kcal/mol Å. It is critical to have many, independent, well-equilibrated initial configurations of the system to be simulated: as the polymer is held together by covalent bonds, the relaxation of the chain is determined by the slowest moving segments along the polymer. Even though mobile segments are expected to exist in large numbers [31], they will be bonded to portions of the polymer that remain "frozen" for timescales vastly longer than what is accessible by MD. Therefore, the only realistic way to explore a large portion of the configurational space is to start with many independent initial system conformations. Accordingly, we used 10 independent initial configurations for each copolymer/surface modifier system, and all energetic values

reported are calculated through NVT ensemble averages of productive MD runs starting from distinctly different initial system configurations. The usage of 10, diverse initial configurations for each simulated system is hence essential, because the relaxation time of both the surfactant molecules and the copolyester chains reach far beyond the time period simulated in each MD run.

After each component was modeled (montmorillonite platelet, surfactant and copolymer), the overall system was built; following Theng [10], each organic compound was oriented perpendicularly to the xy-plane of the mineral, and positioned just above the corresponding magnesium ion but in such a way that the dispersive terms of the van der Waals forces were favored over the repulsive ones.

To generate a proper surface, the lattice constant c of the MMT cell with 6 intercalated surface modifier molecules on one side was extended to 125–150 Å, depending on the length of the organic compound and the polymer molecules. The closest distance of a part of the macromolecule to the organic molecule was around 5 Å. According to previous experience [18,19] this should ensure that the copolyester chain is attracted to the surfactant-MMT surface by favorable non-bonded interactions but, at the same time, it is far away enough so that its initial conformation hardly affects the equilibrium states of the system. Further, $c = 125–150$ Å assures that the polymer molecule does not interact with the K^+ surface of the nearest-neighbor platelet. In other words, even if the model is 3-D periodic, there are no interactions between the periodic images in the z-direction, creating a pseudo 2-D periodic system [32].

Isothermal-isochoric (NVT) MD experiments were run at 350 K, 50 K above the highest experimentally determined glass transition temperature for the BT/TDET 80/20 [16]. The solid surface atoms were constrained to their equilibrium positions via harmonic springs, which allowed for thermal vibrations; comparative studies with completely immobilized solid atoms did not reveal any differences in the results discussed therein. The Newton atomic equations of motion were integrated numerically by the Verlet leapfrog algorithm [33], using an integration step of 1 fs. Temperature was controlled via weak coupling to a temperature bath [34] with coupling constant $\tau_T = 0.01$ ps. Each MD run was started by assigning initial velocity for the atoms according to a Boltzmann distribution at $2 \times T$. It consisted in an equilibration phase, during which system equilibration was monitored by recording the instantaneous values of the total, potential and non-bonded energy, and in a data collection phase, which was extended up to 300 ps.

For the calculation of the binding energy, we considered the potential energy of the global system E_{tot} as given by the following summation:

$$E_{\text{tot}} = E^{\text{MMT}} + E^{\text{poly}} + E^{\text{surf}} + E^{\text{MMT/poly}} + E^{\text{MMT/surf}} + E^{\text{poly/surf}} \quad (1)$$

in which the first three terms represent the energy of MMT, copolyester and surfactant (consisting of both valence and non-bonded terms), and the last three terms are the interactions energies between each of two component pairs (made up of non-bonded terms only). By definition the binding energy is the negative of the interaction energy.

In order to compute the binding energy between the montmorillonite and the polymer matrix, $E_{\text{bind}}^{\text{MMT/poly}} = -E^{\text{MMT/poly}}$, the corresponding MMT/copolyester assembly was created from the global system by removing the surfactant molecules from the optimized conformation, and the corresponding total energy $E^{(\text{MMT,poly})}$ was calculated without further minimization. Then, the MMT platelet and the K^+ cations were removed, and the corresponding energy of the isolated macromolecule E^{poly} was computed. Finally, by deletion of the polymer molecule from the MMT/copolyester ensemble, the remaining energetic term for MMT, E^{MMT} could be obtained. Consequently, the binding energy between the polymeric matrix and the mineral can be calculated according to the following relationship:

$$E_{\text{bind}}^{\text{MMT/poly}} = -E^{\text{MMT/poly}} = -\left(E^{\text{MMT}} + E^{\text{poly}} - \text{E}^{\text{MMT,poly}}\right) \quad (2)$$

In quite an analogous fashion, the binding energies between the MMT and the surfactant, and between the copolyesters and the surfactant, can be calculated as:

$$E_{\text{bind}}^{\text{MMT/surf}} = -E^{\text{MMT/surf}} = -\left(E^{\text{MMT}} + E^{\text{surf}} - E^{(\text{MMT/surf})}\right) \quad (3)$$

$$E_{\text{bind}}^{\text{poly/surf}} = -E^{\text{poly/surf}} = -\left(E^{\text{poly}} + E^{\text{surf}} - E^{(\text{poly/surf})}\right) \quad (4)$$

The estimation of the molecular surface areas and volumes of the organic surface modifiers was performed via the Connolly dot algorithm [35,36], corrected to account for quantum effects using the method proposed by Rellick and Becktel [37]. In this way, no assumption was made about the value of the radii of individual atoms or groups of atoms [38].

RESULTS AND DISCUSSION

To unveil the conformation of the molecules close to the clay surface, we first report three snapshots

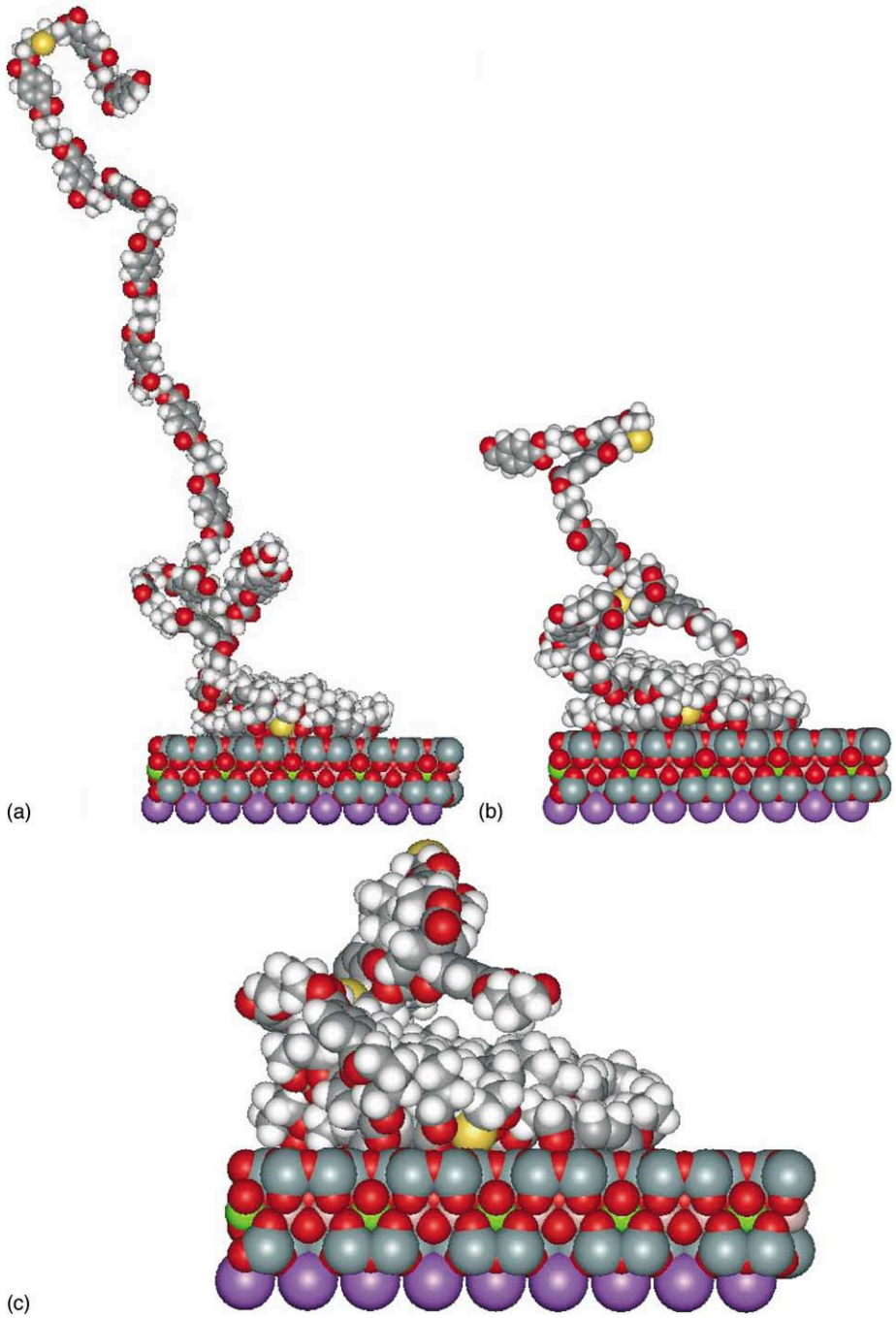

FIGURE 2 Three frames extracted from a MD trajectory at $T = 350\,K$ of a system made up by a pristine MMT platelet and a single copolymester chain of composition BT/TDET 80/20 mol%: (left), 0 ps; (middle), 150 ps and (right), 300 ps.

(0, 100 and 300 ps) taken from a MD simulation at $T = 350\,K$ of a system made up by a pristine MMT platelet and a single copolymer chain, composed by 80 mol% of BT and 20 mol% of TDET (Fig. 2).

In harmony with our previous experience [19], the energy monitoring during the entire MD simulation time revealed that all components of the potential energy were well equilibrated at 50 ps. In particular, the kinetic energy fluctuates around the average value of 800 kcal/mol throughout the data harvesting phase, confirming good temperature control. The potential energy rapidly decreases and remains constant around by virtue of the strongly favorable non-bonded interactions. Indeed, the van der Waals component of the potential energy decreases as the polymer molecule becomes closer to the MMT surface, whereas the highly stabilizing Coulombic term approaches the equilibrium value slightly slower, due to its long-range nature.

Figure 3 shows, as an example, three frames extracted from a MD trajectory at $T = 350\,K$ of a system comprising the copolymer BT/TDET of

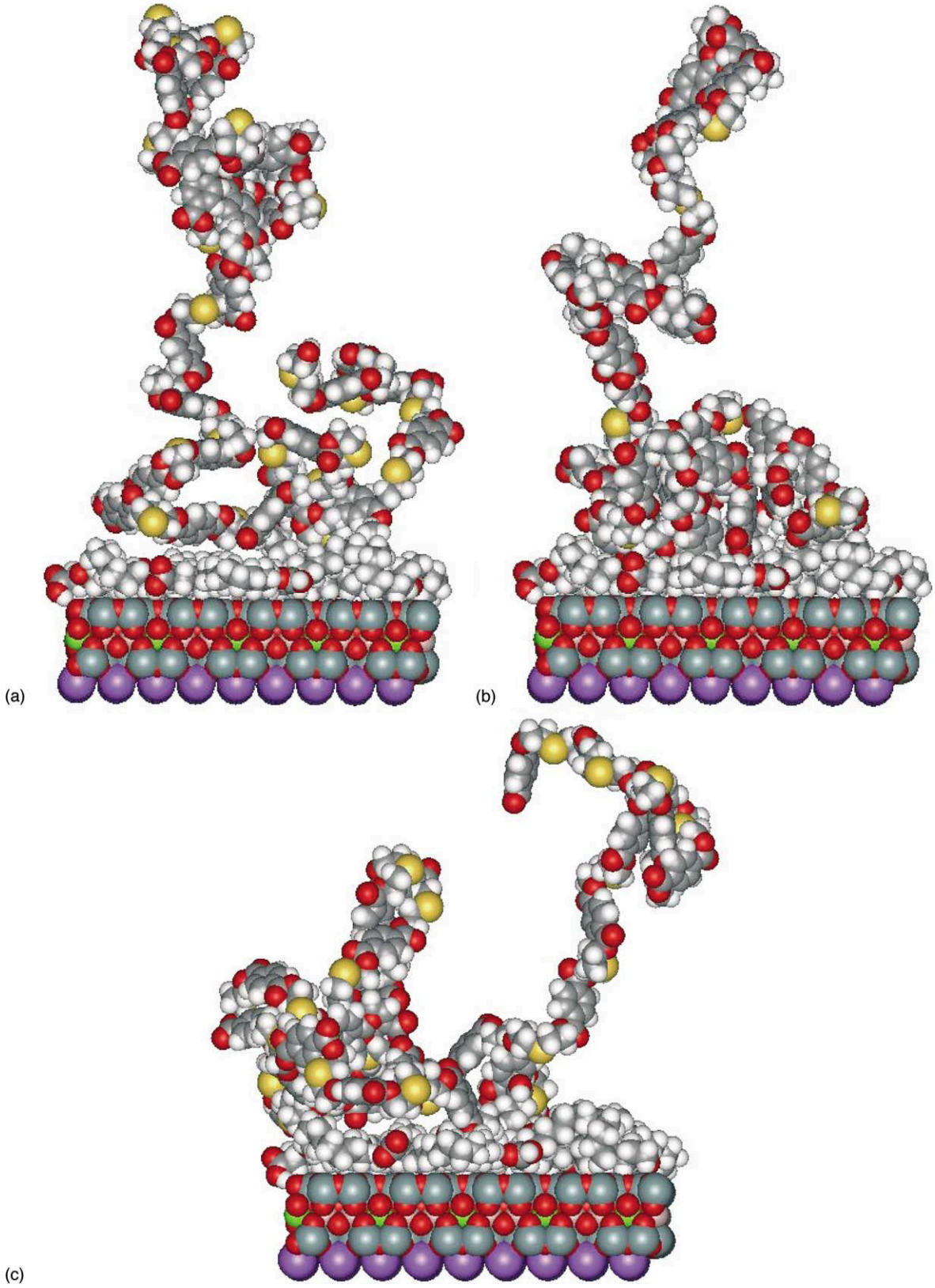

FIGURE 3 Three frames extracted from a MD trajectory at $T = 350\,K$ of a system comprising the copolymer BT/TDET of composition 20/80 mol% and a MMT platelet exchanged with SAc. (left), 0 ps; (middle), 150 ps and (right), 300 ps.

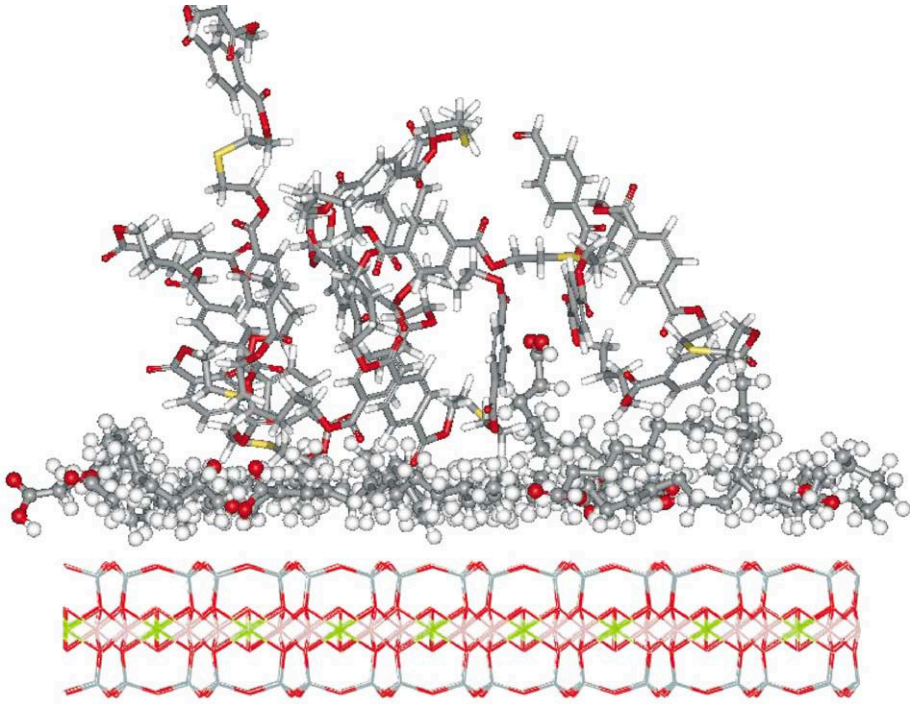

FIGURE 4 Close-up of the snapshot at 150 ps in Fig. 3 near the MMT surface. The mineral is represented by line model, the surfactant by stick-and-ball model and the copolymer by cylinder model.

composition 20/80 mol% and a MMT platelet exchanged with stearic acid (SAc): as the simulation progresses, the surfactant chains flatten onto the clay surface and cover it, within approximately 30 ps elapsed time, and the copolymer molecule docked on top of them within the first 70 ps. An analogous situation has been detected for the other two copolymer composition and for all surfactant considered.

Figure 4 is a close-up of the 200 ps snapshot shown in Fig. 3, using different representations for the SAc, the copolymer and the MMT. This picture clearly shows the conformations of the surfactant and the copolymer chain close to the clay platelet. As we can see, the macromolecule collapses onto the surfactant themselves rather than directly on the clay surface, as the organic molecules shield the interactions between the clay and the copolymer, the larger the surfactant the larger the shielding effect. In all cases, the hydrocarbonic portion of the surface modifiers tends to be straight, lying down flat but, by virtue of their dimensions, forcing some parts to stick outwards from the clay surface. This may eventually facilitate the intercalation of the polymer, as the steric hindrance of these groups would prevent the MMT platelets from getting closer together.

The adsorption of the organic compounds on the MMT layer of the clay surface finds its origin in the resulting, favorable electrostatic interactions. Indeed, all carbon atoms are characterized by a positive charge density, while the oxygen on the mineral surface are negatively charged. As long as they are separated by more than the sum of their van der Waals radii, interactions between the MMT oxygen and the surfactant carbon atoms are always attractive, being mainly electrostatic and secondarily van der Waals.

As explained in the former section, the self- and interaction energies, followed by the binding energy, were calculated from the equilibrium conformation of the corresponding systems. Table II summarizes these results.

Quite generally, three different behaviors can be highlighted: the binding energy between the copolymers and the surfactants decreases in an almost linear fashion with increasing surfactant molecular volume, *V*. Therefore, in principle, smaller organic surface modifiers should provide more efficient interfaces that larger ones, as displayed in Fig. 5 for the copolymer BT/TDET 80/20 mol% as an example. On the other hand, $E_{\text{bind}}^{\text{poly/surf}}$ and $E_{\text{bind}}^{\text{MMT/surf}}$ both increase with *V*, although with a different dependency (Fig. 5). Moreover, the results in Table II seems to indicate that, as the concentration of the TDET unit in the copolymer is increased, the presence of a –SH moiety in the surface modifier becomes significantly and positively manifest.

Since the organic compound shields the interactions between the copolymer and the clay, the systems composed by pristine MMT and the different copolymers are characterized by the highest binding energy, as expected. According to this finding, nanocomposites obtained from untreated clays by, for instance, *in situ* polymerization, should,

TABLE II Binding energies calculated from simulation (see text), and estimated molecular areas and volumes of the surfactants

Chemical formula	$E_{bind}^{MMT/poly}$	$E_{bind}^{poly/surf}$	$E_{bind}^{MMT/surf}$	$E_{bind}^{MMT/poly}$	$E_{bind}^{poly/surf}$	$E_{bind}^{MMT/surf}$	$E_{bind}^{MMT/poly}$	$E_{bind}^{poly/surf}$	$E_{bind}^{MMT/surf}$	*SA* (Å^2)	*V* (Å^3)
Pristine	336.8			300.1			283.6				
$C_{12}H_{27}N$	105.1	133.4	447.0	94.2	122.1	449.8	80.1	119.2	452.8	306	226
$C_{18}H_{39}N$	35.3	202.5	509.4	30.1	199.0	511.6	26.4	180.6	516.6	430	327
$C_{12}H_{24}O_2$	108.7	143.5	422.3	100.1	134.5	430.1	94.7	118.2	433.7	301	224
$C_{18}H_{36}O_2$	33.6	205.3	500.5	26.6	199.3	501.7	23.5	182.5	504.4	429	326
$H_2NC_{12}H_{23}O_2$	100.4	149.5	442.6	89.3	137.3	444.2	80.1	130.5	449.1	316	235
$H_2NC_{18}H_{35}O_2$	34.7	196.4	514.7	23.8	188.4	517.3	28.6	183.1	521.4	445	338
$HSC_{12}H_{23}O_2$	89.1	156.8	453.3	81.3	163.1	458.8	79.2	168.9	462.8	322	243
$HSC_{18}H_{35}O_2$	35.8	200.3	510.8	22.3	205.1	514.3	28.4	210.5	518.7	451	345
$HSC_{12}H_{26}N$	88.3	162.1	462.1	77.1	170.2	467.1	75.1	177.8	474.1	328	244
$HSC_{18}H_{38}N$	32.4	211.1	513.6	26.7	215.8	517.3	22.4	222.6	522.2	451	345
$C_{16}H_{30}NONH_2$	55.6	179.7	488.3	50.0	169.3	491.8	46.1	161.9	496.1	386	298
$C_{22}H_{42}NONH_2$	22.6	224.3	522.4	20.0	219.6	527.7	17.3	211.1	533.3	514	398
$C_{16}H_{30}NOCOOH$	41.1	198.6	500.2	37.2	191.1	506.2	30.2	185	510	399	312
$C_{22}H_{42}NOCOOH$	18.8	253.7	533.3	15.1	244.9	538.4	11.8	238.8	542.8	533	414
$C_{16}H_{30}NOSH$	44.5	188.5	490.1	40.7	195.1	499.1	33.8	200.4	503.7	390	304
$C_{22}H_{42}NOSH$	19.9	245.4	512.9	15.5	253.8	520.0	10.9	258.4	524.6	521	405

Second, third and fourth column: BT/TDET 80/20 mol%; fifth, sixth and seventh column: BT/TDET 50/50 mol%; eighth, ninth and tenth column: BT/TDET 20/80 mol%.

in principle, present the best mechanical properties. This was experimentally verified for nylon-6,6 [39].

It is not clear, however, whether the binding energy between the clay and the copolymers alone is sufficient to determine the fracture toughness or the breaking strength. Since the surfactant molecules adsorb onto the clay surface, it may be more sensible to resort to the sum of $E_{\text{bind}}^{\text{MMT/poly}}$ and $E_{\text{bind}}^{\text{poly/surf}}$ as a better measure of fracture toughness or a surface energy contribution. Thus, Fig. 6 displays, as an example, the dependence of this sum on V again in the case of the copolymer BT/TDET 20/80 mol%. Since the increase in $E_{\text{bind}}^{\text{poly/surf}}$ with V is smoother than the decrease of $E_{\text{bind}}^{\text{MMT/poly}}$ with the same quantity (Fig. 5), the sum still basically decreases with increasing surfactant molecular volume. However, the differences in the binding energies among the different surfactants are sensibly reduced.

The usefulness of a polymer in many applications is largely determined by its predominant failure mechanism under the conditions of application. It is, therefore, very important to be able to predict, even at first approximation, the failure mechanism of polymeric specimens as a function of the structure of the polymer, the processing conditions used in the manufacture of the specimens, and the test conditions. This is clearly a formidable task; nonetheless, at this point, some qualitative interpretations based on simple assumptions about the relationship between fracture mechanics of the considered systems and the simulated quantities can be proposed.

The discipline of fracture mechanics is based on the premise that all materials contain flaws, and that fracture occurs by stress-induced extension of these defects. According to the fundamental principles on polymer large strain behavior, a crack will grow only if the total energy of the polymer is lowered thereby. That is to say, the elastic strain energy, which is relieved by crack growth, must exceed the energy of the newly created surfaces. The relation derived between the crack size and failure stress is known as Griffith criterion:

$$s_{\text{f}} = \left(\frac{2\gamma Y}{pa}\right)^{1/2} \tag{5}$$

where s_{f} is failure stress, based on the initial cross-section, a is the crack depth, Y is the tensile (Young's) modulus and γ is the surface energy of the solid material. This equation applies to completely elastic fractures: all the applied energy is consumed in generating the fracture surface. Real materials are very seldom completely elastic, however, and a more general application of this concept allows for additional energy dissipation in a small plastic deformation region near the crack tip. With this

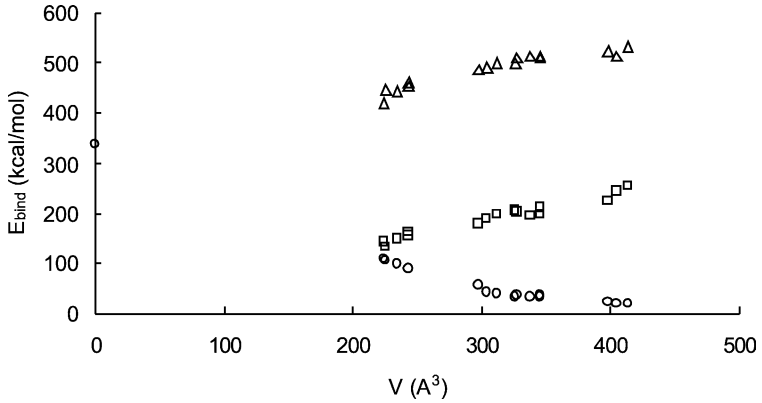

FIGURE 5 Predicted E_{bind} vs. surfactant molecular volume, V, for the copolymer BT/TDET of composition 80/20 mol%. (○), $E_{\text{bind}}^{\text{MMT/poly}}$; (□), $E_{\text{bind}}^{\text{poly/surf}}$; (?), $E_{\text{bind}}^{\text{MMT/surf}}$.

amendment, Eq. (5) is applicable with the 2γ term replaced by G, the strain energy release rate, which includes both plastic and elastic surface work done in extending a preexisting crack:

$$s_{\text{f}} = \left(\frac{YG}{pa}\right)^{1/2} \tag{6}$$

The general equation to describe the applied stress field around a crack tip is:

$$s = \frac{K}{(pa)^{1/2}} \tag{7}$$

where K is the stress intensity factor and s is the local stress. Equation (7) applies at all stresses, but the stress intensity reaches a critical value, K_{c}, at the stress level where the crack begins to grow. K_{c} is a material property, called the fracture toughness, and the corresponding strain energy release rate becomes the critical strain energy release rate, G_{c}.

If we assume that the MMT platelets are fully dispersed within the polymeric matrix, then Y is the same for all the surfactants at the same silicate volume fraction present. As long as the initial crack length is the same, the breaking strength is proportional to the fracture toughness K_{c}. Thus, in the following discussion, we assume that the binding energies calculated by simulation correspond to K_{c}. If fracture is assumed to initiate at the copolymer–clay interface, followed by catastrophic failure of the entire nanocomposite structure, the value of the binding energy between copolymer-6 and MMT can be regarded as representative of K_{c}.

Since, in our case, $E_{\text{bind}}^{\text{MMT/poly}}$ for the clay treated with the smallest surfactant is approximately 5–7 times larger than that of the biggest organic modifier, depending on the copolymer composition (Table II), its breaking strength would also be expected to be higher, on the basis of Eq. (7); moreover, it would be higher than the pristine polymeric material. On the other hand, if a fracture initiates at the interface of both copolyester–clay and copolyester–surfactant, it is the sum of $E_{\text{bind}}^{\text{MMT/poly}}$ and $E_{\text{bind}}^{\text{poly/surf}}$ that relates to K_{c}. According to the values reported in Table II, the breaking strength improvements for the smallest surfactant-treated clay and pristine clay is then attenuated in comparison with the first case, though still higher than the neat copolymer, for all copolymer compositions considered. All other

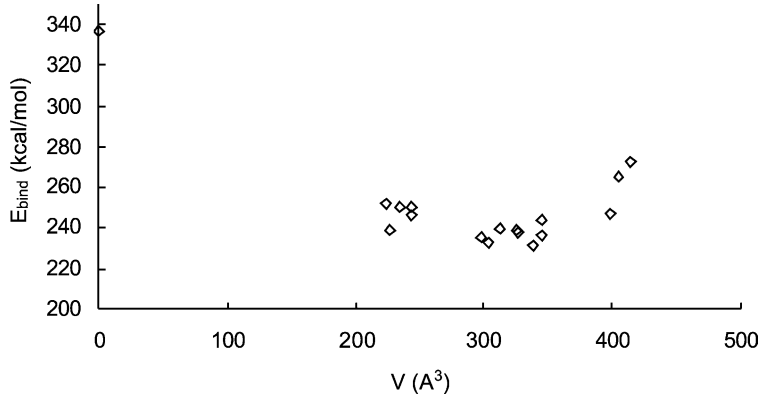

FIGURE 6 Sum of $E_{\text{bind}}^{\text{MMT/poly}}$ and $E_{\text{bind}}^{\text{poly/surf}}$ vs. surfactant molecular volume, V.

intermediated surfactants also yield breaking strength similar to pristine clay.

Fracture toughness and interfacial strength also depend on the polymer crystal size, inhomogeneous stresses and relative orientation of the MMT platelets. With the final goal of improving mechanical properties, crystal sizes can be decreased by using a nucleating agent or resorting to fillers like glass fibers. Since, however, none of them has resulted in improved toughness and strength as much as found in PCNs. Thus, it seems that crystallite size and inhomogeneous stresses produced by large fillers are of secondary importance.

The large aspect ratio of the platelets makes the platelets align parallel to nematic liquid crystals. The spacing between that would be of the order of 100 nm, assuming uniform dispersion. Accordingly, the conditions adopted in our simulations correspond to dilute limit, and effects due to relative orientation are outside the scope of the current study.

CONCLUSIONS

The major findings of this simulation work on random poly(butylene terephtalate-*co*-thiodiethylene terephtalate)-clay nanocomposites can be summarized as follows. First, the energy of binding between the polymeric matrix and the montmorillonite platelet shows a decreasing trend with increasing molecular volume, V, of the organic compounds considered as surfactant, independent of copolymer composition; on the other hand, both the binding energy between the copolymers and the surfactants, and between the surfactants and the montmorillonite increase with increasing V, although with a different slope. Shorter hydrocarbonic chains are more effective in producing favorable binding energies with respect to longer ones, and the substitution of hydrogen atoms with other moieties, such as $-NH_2$, $-COOH$ or $-SH$ generally results in a greater interaction of the surfactant with the polymer. In particular, in the case of a copolymer with the highest sulfur content, the presence of a $-SH$ group in the organic surface modifier becomes positively effective. Finally, under the hypothesis that the clay platelets are uniformly dispersed within the polymer matrix, the pristine clay still yields a high interfacial strength between MMT and the copolymers.

Acknowledgements

This work was supported financially by the Italian Ministry for University and Research (MIUR, Rome, Italy—PRIN 2001 to M. Fermeglia) and by the University of Trieste (Trieste, Italy—Special Grant for Research to S. Pricl and M. Fermeglia). Both are gratefully acknowledged.

References

[1] Giannelis, E.P. (1998) "Polymer-layered silicate nanocomposites: synthesis, properties and applications", *Appl. Organometal. Chem.* **12**, 675.
[2] LeBaron, P.C., Wang, Z. and Pinnavaia, T. (1999) "Polymer-layered silicate nanocomposites: an overview", *Appl. Clay Sci.* **15**, 11.
[3] Alexandre, M. and Dubois, P. (2000) "Polymer-layered silicate nanocomposites: preparation, properties and uses of a new class of materials", *Mater. Sci. Eng.* **28**, 1.
[4] Schmidt, D., Shah, D. and Giannelis, E.P. (2002) "New advances in polymer/layered silicate nanocomposites", *Curr. Opin. Solid State Mater. Sci.* **6**, 205.
[5] Fukushima, Y., Okada, A., Kawasumi, M., Kurauchi, T. and Kamigaito, O. (1988) "Swelling behavior of montmorillonite by poly-6-amide", *Clay Miner.* **23**, 27.
[6] Usuki, A., Kawasumi, M., Kojima, Y., Okada, A., Kurauchi, T. and Kamigaito, O. (1988) "Swelling behavior of montmorillonite cation exchanged for ω-amino acid by ε-caprolactam", *J. Mater. Res.* **8**, 1174.
[7] Kojima, Y., Usuki, A., Kawasumi, M., Okada, A., Kurauchi, T. and Kamigaito, O. (1993) "Synthesis of nylon-6-clay hybrid by montmorillonite intercalated with ε-caprolactam", *J. Polym. Sci. Part A: Polym. Chem.* **31**, 983.
[8] Kojima, Y., Usuki, A., Kawasumi, M., Okada, A., Kurauchi, T. and Kamigaito, O. (1993) "One-pot synthesis of nylon-6-clay hybrid", *J. Polym. Sci. Part A: Polym. Chem.* **31**, 1755.
[9] Kojima, Y., Usuki, A., Kawasumi, M., Okada, A., Fukushima, Y., Kurauchi, T. and Kamigaito, O. (1993) "Mechanical properties of nylon-6-clay hybrid", *J. Mater. Res.* **6**, 1185.
[10] Theng, B.K.G. (1974) *The Chemistry of Clay-Organic Reactions* (Wiley, New York).
[11] Kultys, A. and Podkoscielny, W. (1996) "Polymer containing sulfur in the side chain", *J. Appl. Polym. Sci.* **61**, 1781.
[12] Kultys, A. (1997) "Preparation and properties of polyesters from diphenylmethane-4,4′-di(methylpropionic acid) and aliphatic diols", *J. Polym. Sci. Part A: Polym. Chem.* **35**, 547.
[13] Kultys, A. (1997) "Polyesters containing sulfur V. Preparation and characterization of new polyester-sulfur compositions", *J. Polym. Sci. Part A: Polym. Chem.* **35**, 2231.
[14] Kultys, A. (1999) "Polyesters containing sulfur. VII. New aliphatic–aromatic polyesters for synthesis of polyester-sulfur compositions and polyurethanes", *J. Polym. Sci. Part A: Polym. Chem.* **37**, 835.
[15] Lotti, N., Finelli, L., Milizia, T., Munari, A. and Manaresi, P. (2000) "Preparation and thermal behavior of random copolyesters of thiodipropionic acid", *Eur. Polym. J.* **36**, 929.
[16] Lotti, N., Finelli, L., Siracusa, V., Munari, A. and Gazzano, M. (2002) "Synthesis and thermal characterization of poly(butylene terephtalate-*co*-thiodiethylene terephtalate) copolyesters", *Polymer* **43**, 4355.
[17] Munari, A., personal communication.
[18] Tanaka, G. and Goettler, L.A. (2002) "Predicting the binding energy for nylon 6,6/clay nanocomposites by molecular modeling", *Polymer* **43**, 541.
[19] Fermeglia, M., Ferrone, M. and Pricl, S. (2003) "Molecular modeling of nylon 6/organoclay nanocomposites: prediction of binding energy", *Fluid Phase Eq.*, In press.
[20] van Olphen, H. (1963) *An Introduction of Clay Colloid Chemistry* (Interscience Publishers, New York).
[21] Tsipursky, S.I. and Drite, V.A. (1984) "The distribution of octahedral cations in the 2:1 layers of dioctahedral smectites studied by oblique-texture electron diffraction", *Clay Miner.* **19**, 177.
[22] Sun, H. (1994) "Force field for computation of conformational energies, structures, and vibrational frequencies of aromatic polyesters", *J. Comput. Chem.* **15**, 752.
[23] Sun, H. (1998) "COMPASS: an *ab initio* force-field optimized for condensed-phase applications—overview with details on alkane and benzene compounds", *J. Phys. Chem. B* **102**, 7338.
[24] Fermeglia, M. and Pricl, S. (1999) "Equation of state parameters for pure polymers by molecular dynamics simulations", *AIChE J.* **45**, 2619.
[25] Bayly, C.I., Cieplak, P., Cornell, W.D. and Kollman, P.A. (1993) "A well-behaved electrostatic potential based method using

charge restraints for deriving atomic charges: the RESP model", *J. Phys. Chem.* **97**, 10269.
[26] Cornell, W.D., Cieplak, P., Bayly, C.I. and Kollman, P.A. (1993) "Application of RESP charges to calculate conformational energies, hydrogen bond energies, and free energies of solvation", *J. Am. Chem. Soc.* **115**, 9620.
[27] Hehre, W.J., Radom, L., van Schleyer, P.R. and Pople, J.A. (1986) *Ab Initio Molecular Orbital Theory* (Wiley, New York).
[28] Manias, E. and Kuppa, V. (2002) "Molecular simulations of ultra-confined polymers. Polystyrene intercalated in layered-silicates", In: Vaia, R. and Krishnamoorti, R., eds, *Polymer Nanocomposites* ACS Symposium Series, (Oxford University Press, Oxford) Vol. **804**, Chapter 15, pp 193–207.
[29] Flory, P.J. (1974) *Principles of Polymer Chemistry* (Cornell University Press, Ithaca).
[30] Mattice, W.L. and Suter, U.W. (1994) *Conformational Theory of Large Molecules: The Rotational Isomeric State Model in Macromolecular Systems* (Wiley, New York).
[31] Zax, D.B., Yang, D.-K., Santos, R.A., Hegemann, H., Giannelis, E.P. and Manias, E. (2000) "Dynamical heterogeneity in nanoconfined poly(styrene) chains", *J. Chem. Phys.* **112**, 2945.
[32] Misra, S., Feming, P.D., III and Mattice, W.L. (1995) "Structure and energy of thin films of poly(1,4-*cis*-butadiene): a new atomic approach", *J. Comput. Aided Mol. Des.* **2**, 101.
[33] Verlet, L. (1967) "Computer experiments on classical fluids: I. Thermodynamical properties of Lennard–Jones molecules", *Phys. Rev.* **159**, 98.
[34] Berendsen, H.J.C., Postma, J.P.M., van Gunsteren, W.F., DiNola, A. and Haak, J.R. (1984) "Molecular dynamics with coupling to an external bath", *J. Chem Phys.* **81**, 3684.
[35] Connolly, M.L. (1983) "Solvent-accessible surfaces of proteins and nucleic acids", *Science* **221**, 709.
[36] Connolly, M.L. (1985) "Computation of molecular volume", *J. Am. Chem. Soc.* **107**, 1118.
[37] Rellick, L.M. and Becktel, W.J. (1997) "Comparison of van der Waals and semiempirical calculations of the molecular volumes of small molecules and proteins", *Biopolymers* **42**, 191.
[38] Fermeglia, M. and Pricl, S. (1999) "A novel approach to thermophysical properties prediction for chloro-fluoro-hydrocarbons", *Fluid Phase Eq.* **21**, 166.
[39] Goettler, L.A., Lysek, B.A. and Powell, C.E. (1999) WO 99/41299.